Pattern Analysis and Applications
https://doi.org/10.1007/s10044-022-01099-8

THEORETICAL ADVANCES

Segmentation of breast lesion in DCE-MRI by multi-level thresholding using sine cosine algorithm with quasi opposition-based learning

Tapas Si[1] · Dipak Kumar Patra[2] · Sukumar Mondal[3] · Prakash Mukherjee[4]

Received: 16 August 2021 / Accepted: 5 July 2022

Abstract
In recent times, the high prevalence of breast cancer in women has increased significantly. Breast cancer diagnosis and detection employing computerized algorithms for feature extraction and segmentation can be aided by a physician's expertise in the field. To separate breast lesions from other tissue types in Dynamic Contrast-Enhanced Magnetic Resonance Imaging (DCE-MRI) for segmentation and lesion detection in breast DCE-MRI, radiologists think that multi-level thresholding optimization is efficient. In this article, a lesion segmentation method for breast DCE-MRI using the opposition-based Sine Cosine Algorithm (SCA) is proposed. For breast DCE-MRI segmentation utilizing multilevel thresholding, this work provides an upgraded version of the SCA with Quasi Opposition-based Learning (QOBL). SCAQOBL is the name given to the suggested method in this paper. The Anisotropic Diffusion Filter (ADF) is used to de-noise MR images, and subsequently, Intensity Inhomogeneities (IIHs) are corrected in the preprocessing stage. The lesions are then retrieved from the segmented images and located in MR images. On 100 sagittal T2-weighted fat-suppressed DCE-MRI images, the proposed approach is examined. The proposed method is compared to Opposition-based SCA (OBSCA), SCA, Particle Swarm Optimizer (PSO), Slime Mould Algorithm (SMA), Hidden Markov Random Field (HMRF), and Improved Markov Random Field (IMRF) algorithms. The proposed technique achieves a high accuracy of 99.11 percent, sensitivity of 97.78 percent, and Dice Similarity Coefficient (DSC) of 95.42 percent. The analysis of results is conducted using a one-way ANOVA test followed by a Tukey-HSD test, and Multi-Criteria Decision Analysis (MCDA). The proposed strategy surpasses other examined methods in both quantitative and qualitative findings.

Keywords Breast DCE-MRI · Segmentation · Entropy · Multi-level thresholding · Sine Cosine Algorithm · Opposition-based Learning

1 Introduction

In 2020, 2.3 million women were diagnosed with breast cancer and 685,000 deaths were caused due to breast cancer globally. "As of the end of 2020, there were 7.8 million

Tapas Si, Dipak Kumar Patra and Sukumar Mondal have contributed equally to this work.

✉ Tapas Si
c2.tapas@gmail.com

Dipak Kumar Patra
dpatra11@gmail.com

Sukumar Mondal
sukumarmondal@rnlkwc.ac.in

Prakash Mukherjee
prakashmukherjee25@gmail.com

[1] Department of Computer Science and Engineering, Bankura Unnayani Institute of Engineering, Bankura, West Bengal 722146, India

[2] Department of Computer Science, Raja Narendra Lal Khan Women's College (Autonomous), Midnapore, West Bengal 721102, India

[3] Department of Mathematics, Raja Narendra Lal Khan Women's College (Autonomous), Midnapore, West Bengal 721102, India

[4] Department of Mathematics, Hijli College, Midnapore, West Bengal 721306, India

Published online: 10 August 2022

women alive who were diagnosed with breast cancer in the past 5 years, making it the world's most prevalent cancer" [1]. Biomedical imaging techniques are very useful in the diagnosis, treatment planning, and surgery of breast cancer. Breast cancer is rapidly becoming one of the most ordinary causes of mortality in women around the world. So far, 2.3 million new cases of breast cancer have been discovered, accounting for around $\frac{1}{5}$ of all malignancies. Breast cancer, which accounted for 459410 cases by 2020, is also responsible for 14% of cancer fatalities [2].

Many screening approaches have been utilized in the past for mammography. The most prevalent approach is MRI. The MRI creates an exceptional contrast between similar regions of the breasts' soft tissue, resulting in a clear and crisp breast screen. Breast imaging uses MR images to examine fine details such as malignancies within breast tissues. DCE-MRI of the breast is now widely used to diagnose cancer in the breast. MRI is a major image processing modality in medical diagnosis. MRI modality is used in conjunction with mammography as an appropriate view, especially for women at high risk. Although the sensitivity of MRI of the breast is usually very high, the uniqueness, like all the images, depends on many factors such as the skill of the reader, the use of adequate techniques, and the combination of the patient. MRI is capable of detecting cancers that are not visible in conventional imaging and can be applied to screen high-risk patients. Breast MRI is better today than other imaging methods used to monitor the response to chemotherapy. Some study has shown that when determining breast cancer tumors MRI is more ideal than X-ray, mammography, and sonography. Segmentation of the breast MRI is a major method of image processing in the medical diagnosis of tumors. The breast has three types of tissues : (a) glandular, (b) fibrous, and (c) fatty. Breast MRIs have a maximum of four classes or objects: (i) Background (BA), (ii) Muscle and Skin (MS), (iii) Adipose (AD), and (iv) Glandular (GL). Image processing techniques such as image binarization, image segmentation, and contrast enhancement are routinely employed by radiologists to improve image quality and detect tumor masses.

In this article, a lesion segmentation method for breast DCE-MRI using quasi opposition-based SCA is proposed. SCA [3] is the metaheuristic algorithm developed for function optimization. It's a population-centered optimization strategy. For several situations, the SCA algorithm is an effective, robust, and easy optimization approach [4]. However, there are still significant flaws in how complex practical problems are handled, such as falling into local optima. To address this issue, opposition-based SCA is developed [5, 6]. In study [5], the opposition-based learning (OBL) strategy was used for better exploration in OBSCA and it was used for global optimization. This OBSCA was used for feed-forward neural network (FFNN) training in study [6]. Khrissi et al. [7] developed a SCA-based clustering method for image segmentation. Yan et al. used SCA in multi-level thresholding for underwater image segmentation [8]. Mahender et al. [9] used SCA in multi-level thresholding for lung Computed Tomography (CT) images.

In this article, a new improved SCA by incorporating QOBL, named SCAQOBL, has been proposed for breast lesions segmentation in DCE-MRI. QOBL is the advanced version of the OBL strategy. Our main goal is to use the SCAQOBL to segment breast lesions in DCE-MRI so that we may achieve better results with simple solutions and conduct a more extensive search than existing approaches. In the current study, SCAQOBL is used in Shannon entropy maximization to segment lesions in breast DCE-MRI. The comparative study of results of the proposed method with OBSCA [5], SCA [3], PSO [51], SMA [10], IMRF [11], and HMRF [12] methods is conducted. The Sensitivity, Accuracy, Precision, F-measure, Specificity, Geometric Mean (G-mean), DSC, and False Positive Rate (FPR) are used to evaluate the performance. The statistical analysis [48] method, namely the one-way ANOVA [13] test followed by the posthoc Tukey Honestly Significant Difference (HSD) [14] test is used for statistical analysis of the results. Furthermore, we use Multi-Criteria Decision Making [50] to evaluate overall performance based on the aforementioned criteria. In the experiments, the proposed methodology outperforms the six compared methods.

1.1 Contributions of this article

1. An improved SCA with Quasi Opposition-based Learning (SCAQOBL) is proposed for lesion segmentation in breast DCE-MRI.
2. Experiments are carried out using 100 breast DCE-MRI slices, and the results are investigated considering a set of relevant metrics: accuracy, sensitivity, specificity, precision, geometric-mean, F-measure, false-positive rate, DSC, and convergence graph.
3. The proposed method is compared with OBSCA, SCA, SMA, PSO, IMRF, and HMRF.
4. Discussion about the achieved results with both statistical and multi-criteria decision analysis.
5. The proposed method performs better than other methods.

The remainder of the paper has been organized as bellows: The related works are discussed in Sect. 2. Section 3

describes the background which includes SCA algorithm and opposition-based learning theory. A description of breast MRI dataset is given in Sect. 4. Section 5 describes the proposed method. The proposed segmentation approach based on the SCAQOBL algorithm is presented in this Section. Section 6 describes the experimental setting. Sections 7 and 8 provide the results and discussion respectively. Finally, Sect. 9 provides a conclusion with recommendations for future work.

2 Related works

Many optimization approaches and Evolutionary Algorithms (EA) have been developed for the segmentation of images so far. Segmentation of images using PSO is developed in [15]. The segmentation of Computed Tomography (CT) images is developed using the Genetic Algorithm (GA) in [16].

Adams et al. [17] proposed a high-performance approach, which is widely utilized in the state-of-the-art for medical images. In image segmentation, the Seeded Area Rising (SRG) technique has been proven to have excellent precision [18]. Azmi et al. [19] developed a self-training method for lesion detection in breast MRI. K-Closest of Support Vector Machine (SVM), Neighbors, and Bayesian are 3 supervised techniques that have been developed. Xi et al. [20] used a prior knowledge learning approach on 186 ultrasounds obtained with four distinct types of ultrasound devices. 186 instances, 135 are benign and 51 are cancerous. Their findings showed that the breast lesions segmentation process in experiential learning is both accurate and resilient. A Fuzzy C-Means (FCM) clustering for the segmentation of breast tumors was proposed by Feng et al. [21]. The information extracted from every pixel, such as the strength of its neighbors, is extracted using an FCM approach based on Hausdorff distance in this study. The neighborhood area of each pixel changes and adapts based on shared knowledge between the chosen pixel and neighbors. Euclid and Hausdorff distances are used to compute clustering costs. Patra et al. [22] devised lesion detection in breast DCE-MRI by thresholding and applying Student Psychological-based Optimization (SPBO). The proposed automatic segmentation method has an accuracy of 99.44 percent, a sensitivity of 96.84 percent, and a DSC of 93.41 percent. Si and Mukhopadhyay [23] developed a lesion detection method using Fireworks Algorithm (FWA)-based clustering in breast DCE-MRI. The segmentation approach based on modified hard-clustering with FWA has been developed. The lesions are retrieved from the segmented images. Kar and Si [24] developed a lesion detection method using a Multiverse Optimizer (MVO)-based clustering algorithm of breast DCE-MRI segmentation. A modified hard-clustering with MVO is developed for this purpose. Patra et al. [25] developed a Grammatical Fireworks Algorithm (GFWA)-based lesion segmentation method for breast DCE-MRI. On 25 DCE-MRI slices from 5 patients, the proposed approach is being tested. Ha and Vahedi [26] developed MRI-based breast tumor diagnosis using Improved Deer Hunting Optimization Algorithm based on a feature-based method and hybrid Convolution Neural Network (CNN). The purpose of this work is to use the preprocessing stage to simplify classification. It's also a good idea to use a local binary pattern and Haralick texture to extract features. The accuracy of this method is 98.89 percent as a result of the collected results, indicating its high potential and efficiency. Gihuijs et al. [27] developed a seeds-based region-growing algorithm to segment the lesion from the Region of Interest (ROI) using thresholds. The user, however, needs to pick the seeds manually. Besides, the contrast agent can not act uniformly in the same tissue, which also reduces the precision of threshold-based approaches. As each of the kinetic enhancement curves is an N-D vector, attempts have been made to cluster such curves so that the ROI members of the divided sub-regions are the resulting clusters. Benjelloun et al. [28] introduced Deep Learning in DCE-MRI for automated breast tumor segmentation. They create a U-net fully CNN architecture. On each breast slice, the trained model can handle both detection and segmentation. They used 86 DCE-MRI slices from 43 individuals with local breast cancer, obtained before and after chemotherapy, for a total of 5452 slices. The model is trained and validated on 85 percent and 15 percent of the data, respectively, and achieved a mean score of Intersection Over Union (IoU) of 76, 14 percent. DCE-MRI of the breast utilizing the lesion segment approach proposed by Liang et al. [29]. Automated segmentation is employed in computer-aided diagnosis tools, and this method automatically computes breast density in breast MRI. UNet breast segmentation for Fat-Sat MR slices introduced by Zhang et al. [30] employing transfer learning based on the Non-Fat-Sat model. Deep learning segmentation is accomplished using U-net models with and without TL, with non-fat-sat model initialization of training data. To assess the segmentation results of both the U-net models, the DSC, and accuracy rate depending on all pixels are determined using the ground truth of each example. Wang et al. [31] developed a lesion segmentation method in breast DCE-MRI

using mixed 2D and 3D CNN with Multi-Scale Context (M2D3D-MC). M2D3D-MC achieved 76.4% DSC value.

From the literature survey, it is observed that SCA is never used in MRI segmentation as well as breast DCE-MRI segmentation to date. The use of SCAQOBL for entropy maximization-based breast DCE-MRI segmentation is proposed in this research. The proposed method is discussed in the next section.

3 Background

This section presents basic concepts about SCA and OBL theory.

3.1 Sine cosine algorithm

SCA is an optimization technique that is population-based with a collection of random solutions, seeks the optimization process. Such solutions are determined iteratively by an objective function during iterations. The SCA is based on the Sine-Cosine equation, which can be expressed as in optimization problems for exploration and extraction phases as follows:

$$X_i^{t+1} = X_i^t + r_1 \times \sin(r_2) \times |r_3 P_i^t - X_i^t| \tag{1}$$

$$X_i{}^{t+1} = X_i{}^t + r_1 \times \cos(r_2) \times |r_3 P_i{}^t - X_i{}^t{}_i| \tag{2}$$

where $X_i{}^t$ indicates the location of the current solution in the *i-th* dimension at *t-th* iteration, $r_1/r_2/r_3$ are random numbers, P_i designates the location of the destination points located in the *i-th* dimension, and $||$ is the absolute value.

These combined equations to be applied as follows:

$$X_i{}^{t+1} = \begin{cases} X_i{}^t + r_1 \times \sin(r_2) \times |r_3 P_i{}^t - X_i{}^t| & r_4 < 0.5 \\ X_i{}^{t+1} = X_i{}^t + r_1 \times \cos(r_2) \times |r_3 P_i{}^t - X_i{}^t{}_i| & r_4 \geq 0.5 \end{cases} \tag{3}$$

The planned r_1 parameter is used to direct the next location. To achieve equilibrium between the stage of discovery and exploitation, the During the search process, dynamic fine-tuning of r_1 is done using Eq. (4) as:

$$r_1 = a - t(a/T) \tag{4}$$

where t denotes the present iteration, T denotes the highest number of iterations, and a denotes a constant.

The r_2 parameter is used to determine whether the motion should be toward or away from the goal. r_3 is a random parameter for weighting. The r_4 parameter is a random number in the span [0, 1]. The r_4 parameter is a switching parameter that changes the change between the components of the sine and cosine in Eq. (3). Equations (3) uses conditions $r_4 < 0.5$ and $r_4 \geq 0.5$ for exploration and exploitation processes, respectively. The results of Eqs. (1) and (2) are based on sine and cosine functions. It refers to the region between two solutions in the search space.

3.2 Quasi opposition-based learning

Opposition-based learning (OBL), originally developed by Tizhoosh [32], has proven to be an effective method for some optimization problems and it is incorporated in metaheuristic algorithms for performance improvement [33–35]. SCA begins with an initial population vector, like other metaheuristic algorithms, which is randomly generated when there is no preliminary information available about the solution area. When predefined conditions are met, the phase of evolution terminates. The gap between the ideal solution and the estimate determines the calculation time. By testing the opposite solution at the same time, we can increase the chances of starting with our nearest solution. So as a preliminary solution, the one closest to the solution can be chosen. Indeed, according to probability theory, in 50% of cases the guess is farther to a solution than the opposite guess; for these cases starting with the opposite guess can accelerate convergence. In the current population, the same approach can be extended to any solution, not just to primary solutions.

We need to identify opposite numbers before focusing on opposition-based learning. Let x be a real number in the range $[m, n]$ ($x \in [m, n]$); the opposite number is calculated by

$$\check{x} = m + n - x \tag{5}$$

Let $X(x_1, x_2, \ldots, x_D)$ be a point inside the D dimensional space,

where $x_1, x_2, \ldots, x_D \in R$ and $x_i \in [m_i, n_i]$ $\forall \quad i \quad \in \{1, 2, \ldots, D\}$. The opposite of the X point is described by $\check{X}(\check{x}_1, \check{x}_2, \ldots, , \check{x}_D)$ where

$$\check{x}_i = m_i + n_i - x_i \tag{6}$$

To boost the OBL, quasi opposite points are used instead of opposite points [36]. Let $X(x_1, x_2, ..., x_D)$ be a point in a D-dimensional space with $x_i \in [a_i, b_i]$ be a candidate solution $\forall\ i \in \{1, 2, ..., D\}$ $\check{X}^q(x_1^q, x_2^q, ..., x_D^q)$ should be the quasi-opposite point of p. Assume that $f(x)$ is a fitness function for evaluating candidate optimality. $\check{X}(\check{x}_1, \check{x}_2, ..., \check{x}_D)$ is the polar opposite of $X(x_1, x_2, ..., x_D)$, according to the opposite point description. If $f(\check{X}^q) < f(X)$, then point X is replaced with $\check{X}^q$ if minimization is achieved; otherwise, continue with X. As a result, the point and its quasi-opposite point are both examined at the same time, with the fitter one being evaluated first. In certain cases, the only way to create an initial

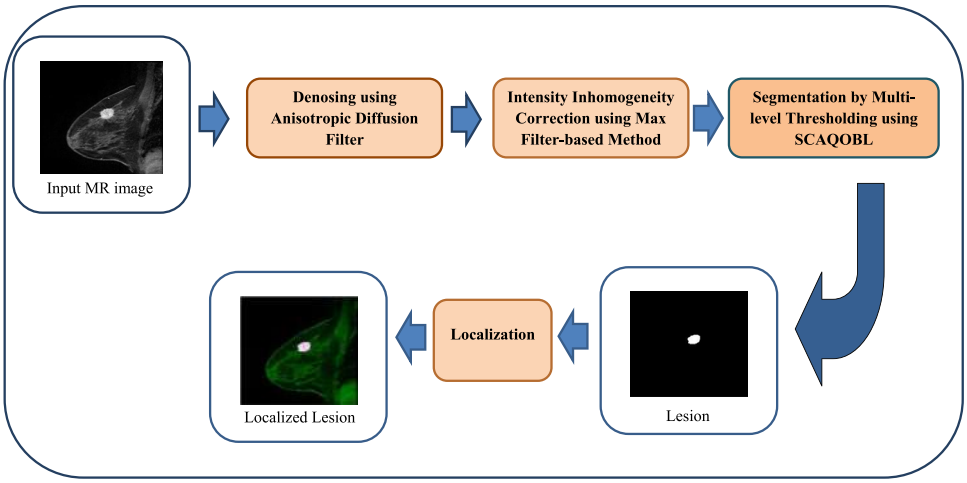

Fig. 1 Outline of the proposed method

population is to use random numbers. Even if there is no priority, the principle of quasi opposition-based learning will help us find more suitable starting candidate solutions.

To calculate the quasi opposition-based solutions, first, we have to calculate the opposite solutions $\check{X}$ using Eq. (6). Then midpoint is calculated using the following equation:

$$C_j = (a_j + b_j)/2 \tag{7}$$

Then finally quasi opposition-based solution is calculated by following equations:

$$\check{X}_j^q = \begin{cases} C_j + (\check{X}_j - C_j) \times rand(0,1) \text{ if } & X_j < C_j \\ \check{X}_j + (C_j - \check{X}_j) \times rand(0,1) & otherwise \end{cases} \tag{8}$$

where $j = 1, 2, \ldots D$, and $rand(0, 1)$ are uniformly distributed random number, D is the number of variables, a_j and b_j are the interval boundaries of the j^{th} variable ($x_j \in [a_j, b_j]$).

4 Breast MRI dataset

Total 100 sagittal T2-weighted fat-suppressed DCE-MRI images of 20 patients are collected from The Cancer Genome Atlas Breast Invasive Carcinoma Collection (TCGA-BRCA) [37, 38] in The Cancer Imaging Archive (TCIA)[1]. Every MRI slice that is larger than 256×256 is shrunk to 256×256. Manual segmentation by a skilled radiologist generates the ground truths, which are regarded as the gold standard [39]. The true value is assigned to the pixels that belong to the lesions in the ground truth images, while the false value is assigned to all other pixels.

5 Proposed method

The following are the three steps of the proposed breast DCE-MRI segmentation method:

1. Preprocessing
2. Segmentation
3. Postprocessing

The proposed method's flowchart is shown in Fig. 1, and each step is described in the following.

5.1 Preprocessing

The visual quality of MRI plays a critical role in appropriately diagnosing treatment, which can be harmed by noise present throughout the acquisition process. The noise in MRI affects both clinical diagnostic functions and the segmentation process [40]. The Anisotropic Diffusion Filter (ADF) [40] is used to de-noise the MR images. An ADF is a technique for eliminating noise without affecting significant portions of the image's content. In [41], ADF is similar to an operation that creates a scale area, in which an image created by a diffusion process develops a parameterized family of increasingly obscure images. In this evolutionary operation, the beginning image is linearly and spatially transmuted. ADF is a generalization of this single action: it generates a spate of parameterized images, but each output image activates the localized content of the starting image, which is a mix of the initial and filter images. The presence of IIHs in MR images also complicates the segmentation process. In an MRI, IIHs are the smooth intensity changes within a previously homogeneous region [42]. The IIHs are corrected using a Max filter-based method [42].

[1] https://wiki.cancerimagingarchive.net/display/Public/TCGA-BRCA.

5.2 Segmentation

The goal of Entropy Maximization is to increase the number of homogeneous positions between them. To avail the pixel frequency in the image, the image histogram is determined. The entropy value is then calculated using pixel frequencies from histograms. The intended solutions are integer numbers in the [0, 255] span, because the image has grey values between 0 and 255.

Shannon entropy [43] is used in this work. This principle is applied to decide the amount of knowledge shown by any data in a probabilistic manner. Let's say an image has homogeneous $(k+1)$ regions and k grey threshold measures at $t_1, t_2, t_3, \cdots, t_k$.

$$h(i) = \frac{f_i}{N} \qquad i = 0, 1, 2, \cdots, 255$$

where $h(i)$ indicates normalized frequency, f_i indicates the frequency of i^{th} gray level, and N is the total number of pixels in the image.

The Shannon Entropy Function is calculated as follows:

$$\begin{aligned} H = &- \sum_{i=0}^{t_1} P_{1i} \ln(P_{1i}) - \sum_{i=t_1+1}^{t_2} P_{2i} \ln(P_{2i}) \\ &- \cdots - \sum_{i=t_k}^{255} P_{ki} \ln(P_{ki}) \end{aligned} \tag{9}$$

$$\text{where, } P_{1i} = \frac{h(i)}{\sum_{i=0}^{t_1} h(i)} \qquad \text{for } 0 \le i \le t_1,$$

$$P_{2i} = \frac{h(i)}{\sum_{i=t_1+1}^{t_2} h(i)} \qquad \text{for } t_1 + 1 \le i \le t_2,$$

$$P_{ki} = \frac{h(i)}{\sum_{i=t_k+1}^{255} h(i)} \qquad \text{for } t_k + 1 \le i \le 255.$$

Entropy function H in Eq. (9) is utilized as an objective function and it is maximized using SCAQOBL for optimal threshold values for segmentation.

Proposed SCAQOBL algorithm The SCA algorithm has been used to resolve a wide range of issues and has proven to be a reliable, simple, and effective optimization procedure. However, there are still some flaws in how it addresses complex functional problems like falling into the local optima. An improved SCA algorithm (SCAQOBL) is suggested here to solve these issues. The definition of quasi opposition learning is embedded in the SCA in this section to increase convergence speed and also to boost its ability to handle optimization issues. Initialization and generation jumping based on the opposition are two goal phases that are expanded by the idea of the opposition foundation.

(i) *Opposition-based initialization* First, individuals of population Y are initialized using the following equation:

$$y_{ij} = y^{\min} + (y^{\max} - y^{\min}) \times rand(0, 1) \tag{10}$$

where y_{ij} is the j^{th} element of i^{th} search agent, $[y^{\min}, y^{\max}]$ is the search space range and $rand(0, 1)$ is the uniformly distributed random number.

The opposite population $\check{Y}^q$ is calculated using the QOBL scheme after the population Y of size n is initialized with $\mathcal{D}$ dimensional vectors at generation zero. Unlike an OBL scheme that generates an opposition point $\check{Y}$, QOBL can generate opposite points within the search space. This instance is avoided by randomly initializing the opposite point in between the quasi point Q, and the boundary point that lies in the same direction as the opposite point. By using the scheme of opposition-based optimization, n fittest parameter vectors are selected from $\{Y \cup \check{Y}^q\}$ to go through the evolution process.

(ii) *Generation jumping* In the opposition-based generation jumping phase, the opposite solutions of the original solutions are computed using the QOBL scheme with generation jumping probability P_{gj}. In this phase, an uniformly distributed random number r is generated in the span [0, 1]. If the random number r is less than generation jumping probability P_{gj} then quasi opposition-based solutions are computed and the n best solutions are chosen from original solutions Y and quasi opposition-based solutions $\check{Y}$. If the random number is greater than or equal to generation jumping probability then the basic operations of SCA are performed. So, n fittest individuals selected from $\{Y \cup \check{Y}^q\}$ go to the next generation;

The pseudo-code of the proposed algorithm is presented in Algorithm 1. Opposition-based initialization phase has been implemented in steps 1-5 of Algorithm 1. Generation jumping phase has been implemented in steps 9-11 with an *if* condition in step 8. If this condition becomes fail, then operations of SCA have been performed in steps 13–16.

Table 1 The parameter settings of algorithms

Algorithm	Parameter	Value
SCAQOBL	Swarm size	30
	P_{gj}	0.3
OBSCA [5]	Swarm size	30
SCA [3]	Swarm size	30
PSO [10, 51]	Swarm size (N)	30
	W	0.72984
	C_1	1.49618
	C_2	1.49618
SMA [10]	Swarm size	30
IMRF [11]	Maximum number of iterations	100
HMRF [12]	Maximum iterations in EM	5
	Maximum iterations in MAP	5

5.3 Postprocessing

In this step, the lesions are eventually retrieved from the segmented MR images using the SCAQOBL technique. In DCE-MRI, the pixels belong to the regions of lesions having hyper-intensities. Therefore, the segment labels of the regions of lesions having the highest values, and segmented images are thresholded using the highest segment labels. We have used region filling [44] to improve the lesion segmentation results for all the algorithms. Finally, utilizing the pixel position of the discovered lesions, the lesions are overlaid with the original MR images for localization.

Algorithm 1 SCAQOBL

```
Randomly initiate the population of size n
Compute the fitness of the individuals
Compute the opposite solutions using QOBL
Evaluate the fitness of opposite solutions
Select the best n solutions from original and opposite solutions
t = 0
while (t < T_max) do          ▷ T_max is the maximum number of iterations
    if rand(0,1) < P_gj then
        Generate opposite solutions using QOBL
        Calculate the fitness of opposite solutions
        Select the best n solutions from original and opposite solutions
    else
        Improve the location of search agents using Eq. 4
        Calculate each of the search agents by the objective function
        Improve the best solution calculated so far
        Improve r1, r2, r3, and r4
    end if
    t = t + 1
end while
Return the best result calculated so far as the global optimum
```

Time and Space Complexity Analysis In Algorithm 1, step 1 takes time $\mathcal{O}(n.\mathcal{D})$. Step 2 takes time $\mathcal{O}(n)$ for fitness calculation. Step 3 takes time $\mathcal{O}(n.\mathcal{D})$. Step 4 takes time $\mathcal{O}(n)$. Step 5 takes time $\mathcal{O}(n^2)$. Step 6 takes time $\mathcal{O}(1)$. Steps 8 - 17 take time $\mathcal{O}(n^2)$. Steps 7 - 19 take time $\mathcal{O}(\mathcal{T}_{max}.n^2)$, where $\mathcal{T}_{max}$ is the maximum number of iterations. Putting all together, the time complexity of the proposed SCAQOBL algorithm is $\mathcal{O}(\mathcal{T}_{max}.n^2)$. Space complexity of the proposed algorithm SCAQOBL is $\mathcal{O}(n.\mathcal{D})$.

6 Experimental setup

The parameters of its comparative algorithms are taken from the articles in which they were developed. The parameter settings are given in Table 1. A maximum number of iterations for all the metaheuristic algorithms is set to 100.

The segmentation method was implemented on an environment with Intel® Core™ i3-8130U @ 2.20GHz CPU,

Table 2 Performance metrics

Metric name	equation
Accuracy [22, 49]	(TP + TN)/(TP + FN + TN + FP), TP: True Positive Rate, FP: False Positive Rate, TN: True Negative Rate, FN: False Negative Rate
Sensitivity (recall) [22, 49]	TP/(TP + FN)
Specificity [22, 49]	TN/(TN + FP)
Precision [22, 49]	TP/(TP + FP)
G-Mean [22, 49]	$\sqrt{Sensitivity \times Specificity}$
F-Measure [22,49]	$\frac{2\times recall\times precision}{recall+precision}$
FPR [22, 49]	1- Specificity
DSC [22, 49]	DSC(A,B)=$\frac{2\lvert A\cap B\rvert}{\lvert A\rvert\cup\lvert B\rvert}$, A: segmented image, B: ground truth

Windows 7 Ultimate (64-bit) operating system, RAM 4 GB, and MATLAB 2017b software.

6.1 Performance measurement

It is a difficult task to design or choose an appropriate effectiveness measure of image segmentation. Information relevant to the task, whether diagnostic or interventional, should be provided by the performance assessment. Sensitivity, accuracy, precision, specificity, FPR, G-mean, DSC, and F-measure are some of the parameters used and details of these measures can be obtained from [22, 49]. The definition of each metric is provided in Table 2.

7 Results

Lesion segmentation techniques for breast DCE-MRI are proposed in this study. The noise and IIHs in the MR images make segmentation more difficult. As a result, an ADF is used to remove noise from MR images, and IIHs correction is done during the preprocessing stage. The identical experiments are performed 10 times for a single image because the SCAQOBL technique starts with a randomly initialized population.

7.1 Quantitative results

Over 10×100 findings, the quantitative outcomes of the mean value and standard deviation value of performance evaluation indicators are examined. The novel approaches are evaluated and compared to the traditional OBSCA, SCA, PSO, SMA, IMRF, and HMRF procedures.

The quantitative results of the proposed method compared to six methods are provided in Table 3 and bold-faced results indicate better.

It is observed from Table 3 that the mean accuracy of the proposed method is higher than that of OBSCA, SCA, SMA, PSO, IMRF, and HMRF. SCAQOBL has an accuracy of 99.11%, which is higher than all other approaches. The

Table 3 Mean and standard deviation (in parenthesis) of performance evaluation scores (in %)

Performance Metrics	SCAQOBL	OBSCA	SCA	PSO	SMA	IMRF	HMRF
Accuracy	**99.11**	98.60	98.07	97.36	96.80	96.13	96.60
	(0.0262)	(0.0361)	(0.0465)	(0.0582)	(0.0841)	(0.0741)	(0.0703)
Sensitivity	**97.78**	96.99	95.69	92.78	88.06	87.51	92.69
	(0.0233)	(0.0473)	(0.0829)	(0.0933)	(0.1342)	(0.1458)	(0.1179)
Specificity	**99.15**	98.76	98.22	97.64	96.98	96.40	96.73
	(0.0292)	(0.0445)	(0.0419)	(0.0535)	(0.0681)	(0.0697)	(0.0685)
Precision	**93.32**	92.60	91.86	82.57	80.20	82.64	79.85
	(0.0775)	(0.0759)	(0.0891)	(0.1772)	(0.1276)	(0.2528)	(0.1734)
G-mean	**98.54**	98.16	96.98	94.38	93.55	93.46	92.70
	(0.0412)	(0.0239)	(0.0478)	(0.0708)	(0.0707)	(0.0597)	(0.0931)
F-measure	**94.28**	92.92	91.89	84.45	81.56	82.48	83.68
	(0.0434)	(0.0629)	(0.0742)	(0.1012)	(0.0728)	(0.2128)	(0.1113)
FPR	**0.85**	1.24	1.78	2.36	3.02	3.60	3.27
	(0.0142)	(0.0193)	(0.0185)	(0.0182)	(0.0143)	(0.0128)	(0.0136)
DSC	**95.42**	91.36	88.98	84.24	84.06	83.59	81.84
	(0.0374)	(0.0798)	(0.0763)	(0.0985)	(0.1206)	(0.2125)	(0.2132)

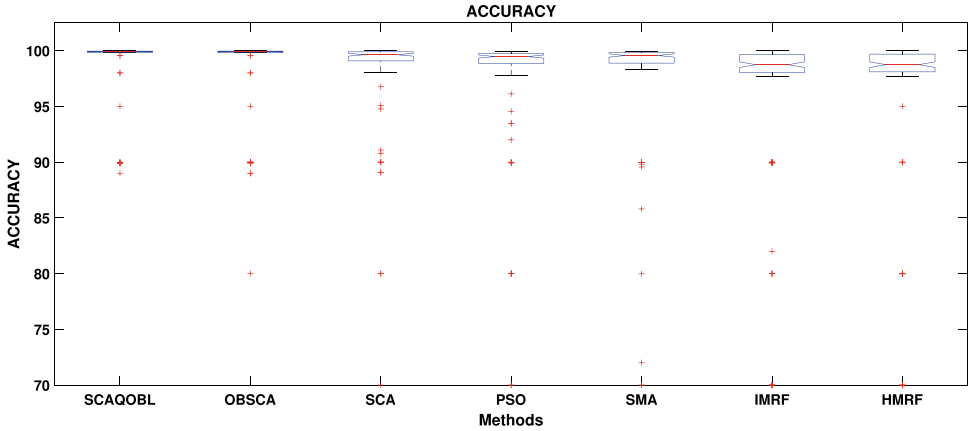

Fig. 2 Boxplot (methods versus Accuracy) of comprehensive classification performance

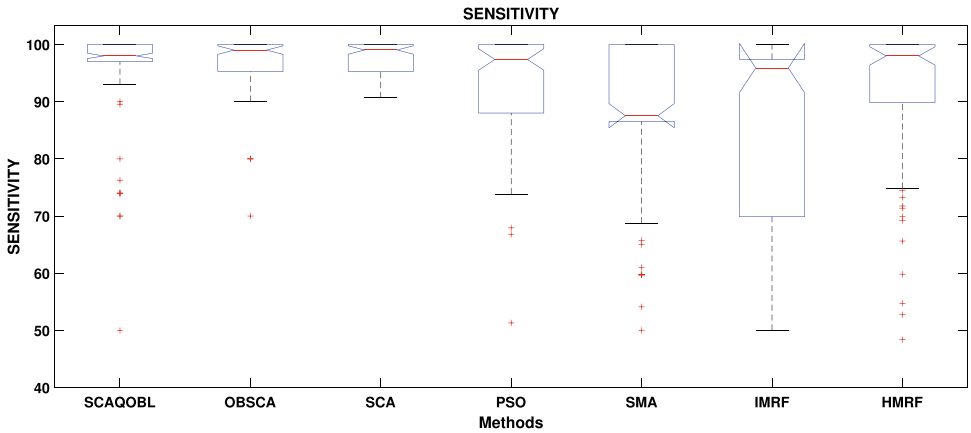

Fig. 3 Boxplot (methods versus Sensitivity) of comprehensive classification performance

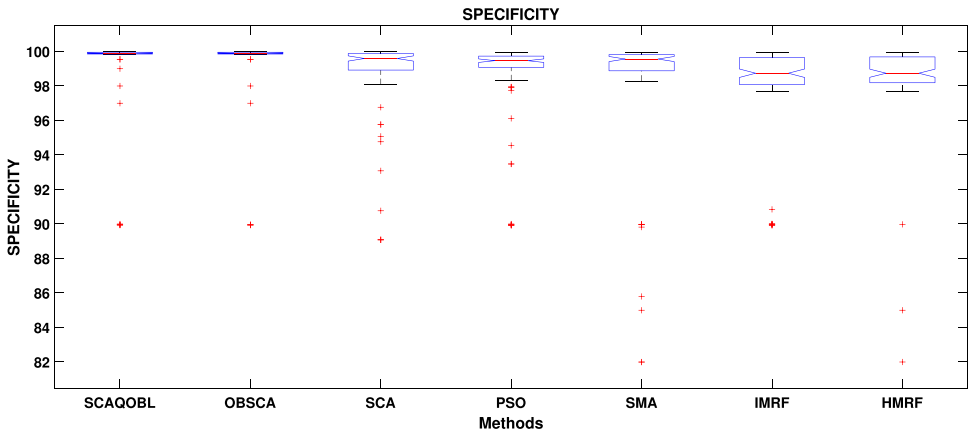

Fig. 4 Boxplot (methods versus Specificity) of comprehensive classification performance

suggested method's mean sensitivity score is 97.78 percent, and its mean specificity score is 99.15 percent, higher than that of the OBSCA, SCA, SMA, PSO, IMRF, and HMRF approaches. The mean precision value for SCAQOBL is 93.32 percent, whereas the mean precision scores for OBSCA, PSO, SCA, SMA, IMRF, and HMRF are 92.60 percent, 91.86 percent, 82.57 percent, 80.20 percent, 82.64 percent, and 79.85 percent, respectively.

The proposed technique outperforms OBSCA, SCA, PSO, SMA, IMRF, and HMRF with a mean G-mean score of 98.54 percent.

The F-measure is used to determine the sensitivity-to-precision trade-off. The proposed technique has a mean F-measure of 94.28 percent, which is significantly higher than OBSCA, SCA, SMA, PSO, IMRF, and HMRF. The

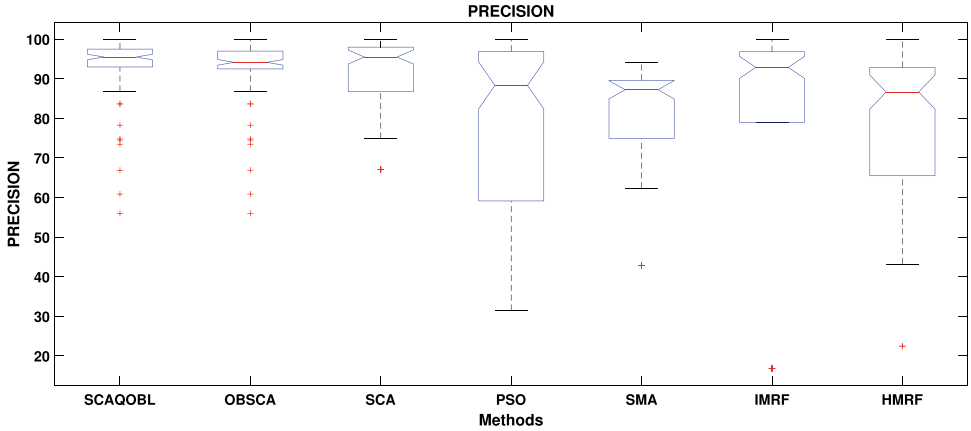

Fig. 5 The boxplot (methods versus Precision) of comprehensive classification performance

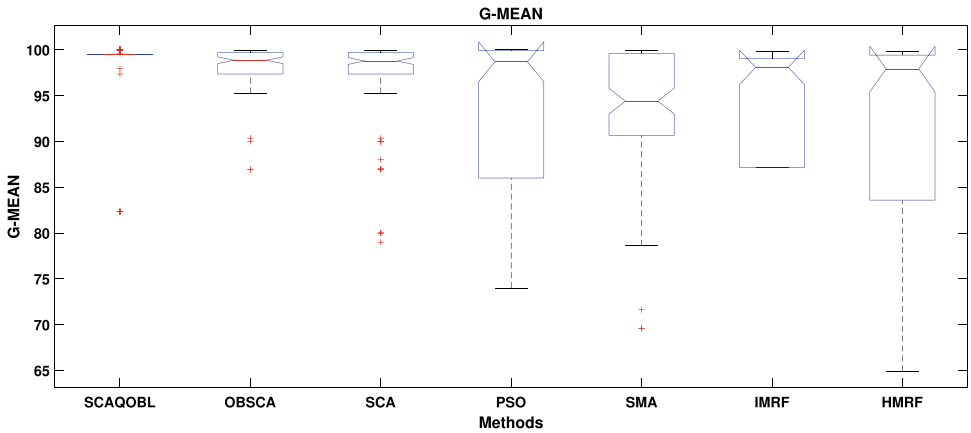

Fig. 6 Boxplot (methods versus G-mean) of comprehensive classification performance

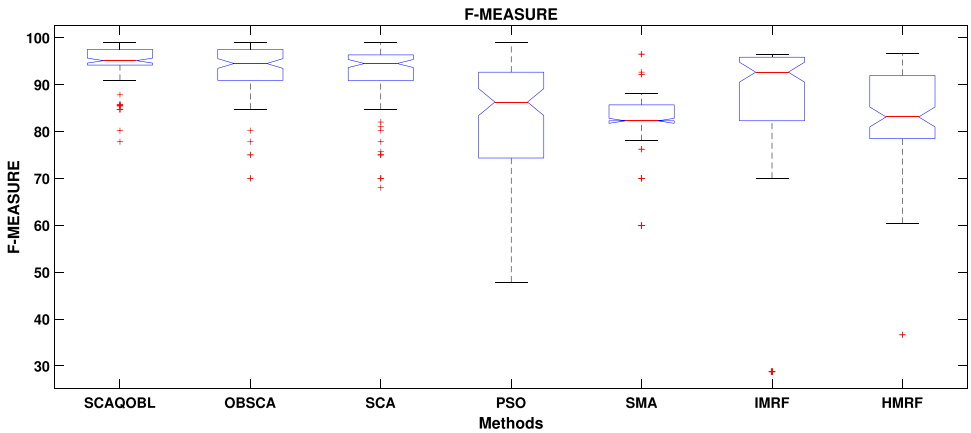

Fig. 7 Boxplot (methods versus F-measure) of comprehensive classification performance

F-measure refers to the precision with which lesion tissues in the breast are classified. The higher this indicator's value, the more likely it is that the SCAQOBL classification can accurately identify lesions in breast MRI.

The false alarm rate is another form of FPR, it determines the proportion of incorrectly labeled negative samples to the total number of negative samples. Because FPR is unaffected by changes in data distribution, both metrics can be used with unbalanced data. The proposed approach (SCAQOBL) has a mean FPR of 0.85 percent, which is significantly lower than OBSCA, SCA, PSO, SMA, IMRF, and HMRF.

The proposed method's mean DSC value is 95.42 percent, which is greater than the methods of OBSCA, SCA, PSO, SMA, IMRF, and HMRF. The higher the DSC value,

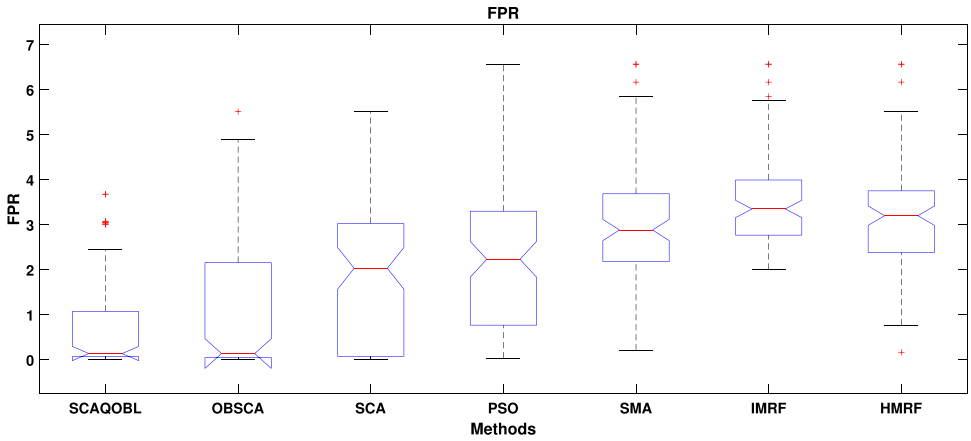

Fig. 8 Boxplot (methods versus FPR) of comprehensive classification performance

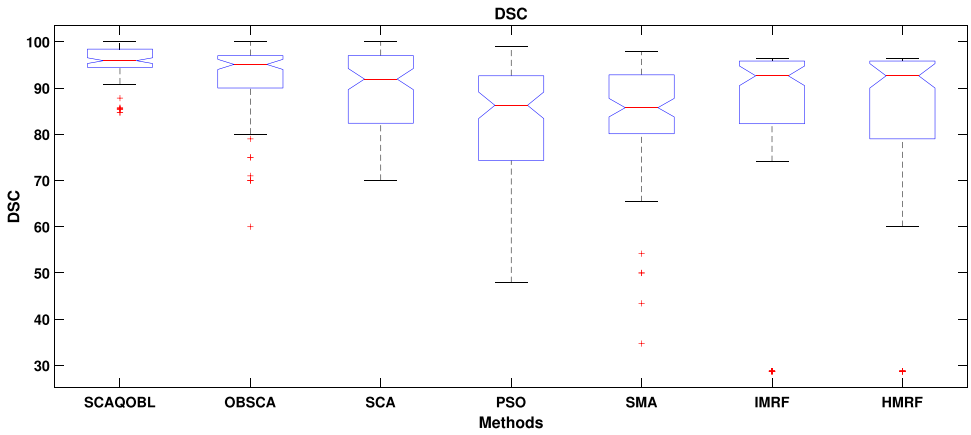

Fig. 9 Boxplot (methods versus DSC) of comprehensive classification performance

the larger the overlap with the segmentation lesions' ground truths. The suggested SCAQOBL-based method outperforms the OBSCA, SCA, PSO, SMA, IMRF, and HMRF in the examination of the given quantitative data.

It's also important to consider the robustness or stability of lesion detection segmentation approaches as the proposed SCAQOBL has random behaviors due to which results are different in different runs. It is calculated over numerous runs in terms of the standard deviation of output variables, with a lower standard deviation indicating higher resilience. Because the standard deviations in Table 3 are less than that of six other approaches, the suggested segmentation procedure is robust for breast lesion detection in DCE-MRI.

A boxplot is a type of chart often used in explanatory data analysis. Box plots visually show the distribution of numerical data and skewness by displaying the data quartiles and averages. Boxplots show the five-number summary of a set of data: minimum score, first quartile, median, third quartile, and maximum score. A boxplot is a graph that shows how the values are distributed in the details. Boxplots, on the other hand, can appear rudimentary when contrasted with a density plot. Figure 2 shows that the proposed SCAQOBL has a greater median classification accuracy result than the other six existing approaches. Because the accuracy results are compacted, the lowest difference and maximum value are quite small. SCAQOBL also has a higher median sensitivity value than the other approaches shown in Fig. 3. The recommended SCAQOBL has a greater median specificity of categorization than the other approaches, as shown in Fig. 4. SCAQOBL also has a higher median precision value than the other approaches shown in Fig. 5. SCAQOBL has a higher median G-mean, F-measure, FPR, and DSC value than competitive methods as observed in Figs. 6,7, 8, and 9, respectively. Furthermore, it is also observed that the median of all performance measured from SCAQOBL is statistically better than others with significance level 0.05.

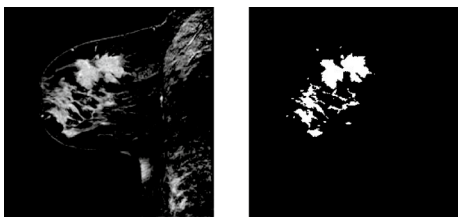

(a) MRI slice (b) Ground truth

Fig. 10 For Patient-1 **a** MR slice, **b** Ground truth

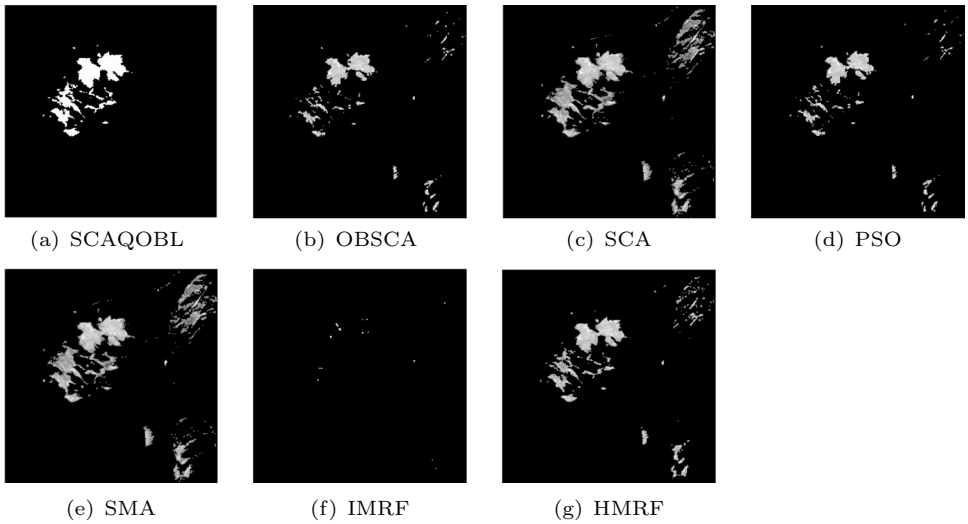

Fig. 11 For Patient-1 **a**–**g** SCAQOBL, OBSCA, SCA, PSO, SMA, IMRF, and HMRF respectively

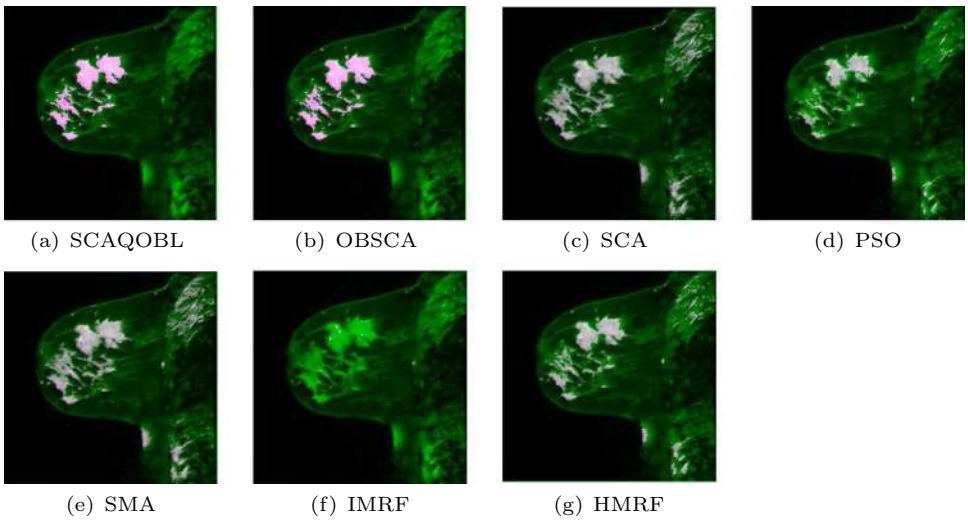

Fig. 12 Localized lesions (bright colored spot) in MR images for patient-1 **a** – **g** SCAQOBL, OBSCA, SCA, PSO, SMA, IMRF, and HMRF, respectively

7.2 Qualitative results

For the validation of this strategy, a total of 100 images of 20 patients are employed. Due to space constraints, only the results for the 1 image of 1 patient is shown from a total of 100 test results. The original MR slice and ground truth image are given in Fig. 10. Figure 11 for patient-1 shows segmented breast lesions using various approaches. The localized lesional images are provided in Figs. 12 for patient 1.

By comparing the ground truth image in Fig. 10b with the SCAQOBL segmented image in Fig. 11a for MRI images of patient-1, it is clear that SCAQOBL has virtually completely segmented the lesion regions. When compared to the ground truth image, the suggested SCAQOBL-based technique performs well in detecting lesions in the image.

It may clearly be shown in Fig. 11b that OBSCA detects some healthy tissues as lesions. When compared to the ground truth image, the OBSCA-based technique does not perform well in detecting lesions in the image.

It may clearly be shown in Fig. 11c that SCA detects certain healthy tissues as lesions. When compared to the ground truth image, the SCA technique does not perform well in detecting lesions in the image.

Table 4 ANOVA Test Statistics based on DSC

Source of Variance	SS	df	MS	F	*p-value*	F-crit.
Between Groups	15319.86	6	2553.309	13.9037	5.76E-15	2.1116
Within Groups	127264.1	693	183.6423			
Total	142584	699				

Table 5 Tukey HSD Test Statistics based on DSC

Sl. No.	Comparison	Comparison with T	Result (Significant at α=0.05)
1	SCAQOBL *vs* OBSCA	4.06 > 3.9895	yes
2	SCAQOBL *vs* SCA	6.44 > 3.9895	yes
3	SCAQOBL *vs* PSO	11.18 > 3.9895	yes
4	SCAQOBL *vs* SMA	11.36 > 3.9895	yes
5	SCAQOBL *vs* HMRF	11.83 > 3.9895	yes
6	SCAQOBL *vs* IMRF	13.58 > 3.9895	yes

Table 6 MCDA rank

Methods	Rank
SCAQOBL	1
OBSCA	2
SCA	3
PSO	4
SMA	5
HMRF	6
IMRF	7

It may clearly be shown in Fig. 11d for MRI slice of patient-1 that PSO detects certain healthy tissues as lesions. When compared to the ground truth image, the PSO-based technique does not perform well in detecting lesions in the image. It may be seen in the SMA segmented image in Fig. 11d that some lesions are not segmented by SMA. When compared to the ground truth image, the SMA-based technique does not perform well in detecting lesions in the image. IMRF detects certain healthy tissues as lesions. In comparison to the ground truth image, this approach does not do well in detecting lesions in the image. Some healthy tissues are segmented by HMRF, as shown in Fig. 11g. These approaches do not perform well in detecting lesions for the images.

7.3 Statistical analysis

Statistical analysis has been conducted based on DSC using one-way ANOVA [13] followed by posthoc test Tukey Honestly Significant Difference (HSD) [14] to validate the segmentation performance. DSC indicates the overlapping ratio of the segmented lesions to the ground truths. The better the performance, the higher the DSC rating. The ANOVA test result is given in Table 4. It is observed from this table that the *p-value* of the ANOVA test is $5.76E-15$ which is less than the significant level at $\alpha = 0.05$. After the ANOVA test, the suggested SCAQOBL method is compared to the other methods using the Tukey HSD statistical test, and the result is presented in Table 5. With a significance threshold of $\alpha = 0.05$, Table 5 shows that SCAQOBL statistically outperforms the other methods.

7.4 Multi-criteria decision analysis

Multi-Criteria Decision Analysis (MCDA) [45] has been conducted using the well-known TOPSIS method and this philosophy is adopted from the study [22, 46]. Multiple criteria are used here, including sensitivity, accuracy, specificity, precision, G-mean, FPR, DSC, and F-measure are all terms for the same thing. Because low FPR numbers imply better, yet greater values of other criteria indicate better, FPR clashes with other criteria. Table 6 describes the ranks obtained from a TOPSIS technique. The SCAQOBL method has the greatest ranking, according to Table 6. The OBSCA approach is then followed by the SCAQOBL method. It's also worth noting that IMRF is near the bottom of the list.

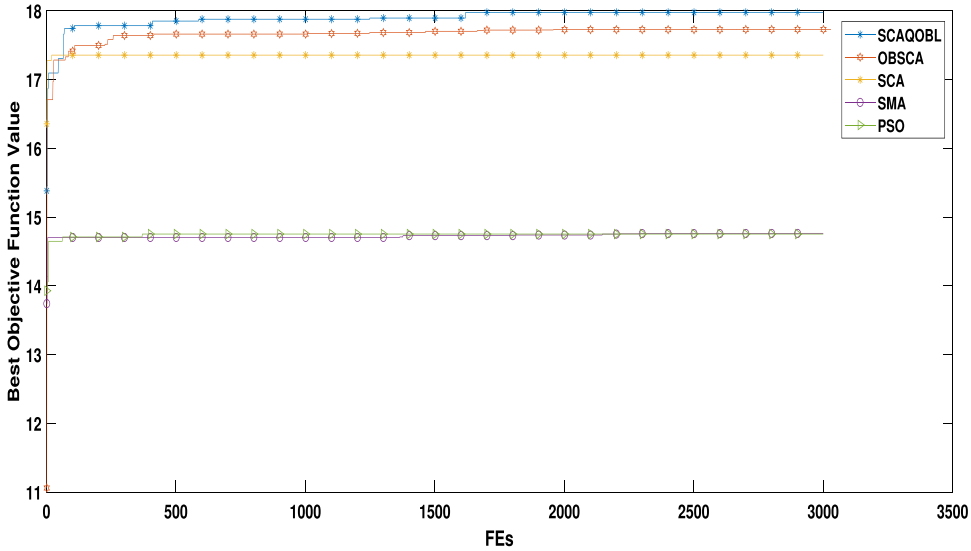

Fig. 13 Convergence graph for MRI slice in Figure 10**a**

7.5 Computational time cost analysis

According to our findings, SCAQOBL's average CPU execution time is 6.3959 seconds. OBSCA takes an average of 5.9114 seconds to execute. SCA takes an average of 2.9114 seconds to execute. The average execution time of PSO and SMA is 2.8809 seconds and 2.9905 seconds, respectively. IMRF takes an average execution time of 2.9245 seconds, while HMRF's average execution time is 2.5954 seconds. When compared to all existing approaches, the proposed method takes a few more times to execute on the CPU, but it performs better in segmentation.

7.6 Convergence analysis

Fig. 13 shows the convergence graphs for the image in Fig. 10a. The entropy values, i.e., best objective function values are displayed against the Function Evaluations (FEs) in graphs. The graph depicts how far the search has progressed in finding the optimum solution. The convergence behavior of SCAQOBL is better than that of other metaheuristic algorithms, as shown by the convergence graphs. After roughly 100 FEs, the convergence graph in Fig. 13 shows that SCAQOBL converges very close to the optimal outcome. SCAQOBL consistently outperforms OBSCA, SCA, SMA, and PSO. SCAQOBL converges with a very close to the best result after around 500 FEs, but OBSCA converges with a very close to the best result after about 1200 FEs, according to the convergence graph demonstrates the SCAQOBL algorithm's superior searching ability for entropy maximization.

Better segmentation performance in breast fat-suppressed DCE-MRI is achieved by SCAQOBL compared to OBSCA, SCA, SMA, PSO, IMRF, and HMRF, according to the above examination of both quantitative and qualitative data. According to the results of the trials, SCAQOBL is efficient and successful in breast lesion segmentation in DCE-MRI.

As evidenced by the foregoing both quantitative and qualitative analysis, the suggested technique based on SCAQOBL outperforms other compared methods in the lesion detection in breast DCE-MRI. Because SCAQOBL has high searching ability and convergence properties, it is effective at determining appropriate threshold values for segmentation.

8 Discussion

In this work, we have proposed an algorithm for breast tumor segmentation. The proposed algorithm uses sagittal T2-weighted fat-suppressed DCE-MRI data and relies on Shannon entropy maximization features. The algorithm is applied to the DCE-MRI dataset, and it gives better results (performance evaluation) than the state-of-the-art methods as shown in Table 3. In the preprocessing step, we applied denoising using ADF, and calculated IIHs using max filter based method. In SCAQOBL, the QOBL scheme is employed in the initialization phase, and the generation jumping phase results in better exploration in the search space than SCA. We have found that basic SCA suffers from premature convergence in local optima due to a lack of diversity in the search space. Hence, we need to improve the SCA to achieve a better quality of solutions. Therefore, we have developed quasi opposition-based SCA namely SCAQOBL in this article. After the denoised image has been obtained, entropy maximization is utilized to determine the suitable threshold values for segmentation. The purpose of increasing the number of homogeneous sites between them is to maximize entropy. The entropy value is then calculated using pixel frequencies from histograms. The objective function, i.e., entropy function is maximized by using the SCAQOBL algorithm. In the postprocessing step, the lesions are eventually retrieved from the segmented MR images using the SCAQOBL technique. We have used region filling to improve the segmentation results for all the algorithms. The statistical analysis method namely, the one-way ANOVA test followed by the post-hoc Tukey Honestly Significant Difference (HSD) test is used for statistical analysis of the results. A boxplot is a graph that shows how the values are distributed in the details. Boxplots, on the other hand, can appear rudimentary when contrasted with a density plot. Figures 2, 3, 4, 5, 6, 7, 8 and 9 show that the proposed SCAQOBL has a greater median classification result than the other six existing approaches.

Furthermore, we use Multi-Criteria Decision-Making to evaluate overall performance based on the aforementioned criteria. In the experiments, the proposed methodology outperforms the six compared methods. The convergence graph demonstrates the SCAQOBL algorithm's superior searching ability for entropy maximization. The quantitative results with both statistical analysis and multi-criteria decision analysis, and qualitative results establish that the proposed lesion segmentation method outperforms other compared methods.

9 Conclusion with potential future works

The goal of this research is to look into and build an efficient method for breast DCE-MRI segmentation to help radiologists diagnose, and treatment. This work describes a SCAQOBL method for multi-level thresholding of breast DCE-MRI to detect lesions. The SCAQOBL algorithm is used to identify the best threshold values by maximizing entropy. On 100 T2-weighted sagittal MR images, the suggested method SCAQOBL is used. The experimental

findings reveal the effectiveness of the suggested technique, which has obtained greater performance in terms of sensitivity, accuracy, f-measure, precision, specificity, DSC, and G-mean when compared to the existing OBSCA, SCA, PSO, SMA, IMRF, and HMRF methods. The average performance of the suggested technique evaluated by the MCDM method is likewise greater based on the given parameters. The proposed approach is effective at detecting lesions in breast DCE-MRI.

In the future, we intend to apply the SCAQOBL-based segmentation method for lesion detection in the MRI of the brain, liver, kidney, soft tissue sarcoma, etc. We also intend to develop enhanced SCAs by incorporating other OBL schemes and applying them in the segmentation of biomedical images. In this work, we have used Shannon entropy for multi-level thresholding. We intend to investigate other entropy like Tsallis entropy, Rényi entropy, Kapur entropy, etc. in the proposed method. Multi-objective SCA (MOSCA) [47] can be applied to segment the breast DCE-MRI as a future work of this study.

Acknowledgements We are thankful for the assistance from the expert radiologists of Auro MRI Centre Private Limited, Tamluk - 721636, West Bengal, India during this research.

Declarations

Conflict of interest Authors declare that there is no conflict of interests.

References

1. World Health Organization (WHO) (2021) Breast cancer https://www.who.int/news-room/fact-sheets/detail/breast-cancer
2. Sung H, Ferlay J, Siegel RL, Laversanne M, Soerjomataram I, Jemal A, Bray F (2021) Global cancer statistics 2020: GLOBOCAN estimates of incidence and mortality worldwide for 36 cancers in 185 countries. CA Cancer J Clin 71:209–249. https://doi.org/10.3322/caac.21660
3. Mirjalili S (2016) SCA: a sine cosine algorithm for solving optimization problems. Knowl Based Syst 96:120–133. https://doi.org/10.1016/j.knosys.2015.12.022
4. Gabis AB, Meraihi Y, Mirjalili S, Ramdane-Cherif A (2021) A comprehensive survey of sine cosine algorithm: variants and applications. Artif Intell Rev. https://doi.org/10.1007/s10462-021-10026-y
5. Elaziz MA, Oliva D, Xiong S (2017) An improved opposition-based sine cosine algorithm for global optimization. Expert Syst Appl 90:484–500. https://doi.org/10.1016/j.eswa.2017.07.043
6. Bairathi D, Gopalani D (2017) Opposition-based sine cosine algorithm (OSCA) for training feed-forward neural networks IEEE 13th International Conference on signal-image technology and internet-based systems 438-444 https://doi.org/10.1109/SITIS.2017.78.
7. Khrissi L, El Akkad N, Satori H, Satori K (2021) Clustering method and sine cosine algorithm for image segmentation. Intel Evol. https://doi.org/10.1007/s12065-020-00544-z
8. Yan Z, Zhang J, Tang J (2020) Sine cosine algorithm for underwater multilevel thresholding image segmentation Global Oceans 2020: Singapore–US Gulf Coast IEEE https://doi.org/10.1109/IEEECONF38699.2020.9389009.
9. Mahender E, Babu CR, Kumar KS (2021) Multi-level thresholding for image segmentation on medical images using multi otsu and sine cosine optimization algorithm. Ann Romanian Soc Cell Biol 5:12305–12316. https://doi.org/10.1007/s12065-020-00544-z
10. Li S, Chen H, Wang M, Heidari AA, Mirjalili S (2020) Slime mould algorithm: a new method for stochastic optimization. Future Gener Computer Syst 111:300–323
11. Azmi R, Norozi N (2011) A new markov random field segmentation method for breast lesion segmentation in mr images. J Med Signals Sens 1:156–164
12. Chatzis SP, Tsechpenakis G (2010) The infinite hidden Markov random field model. IEEE Transactions Neural Netw 21(6):1004–1014
13. Anscombe F (1948) The validity of comparative experiments. J R Statistical Soc 111(3):181–211
14. Tukey JW (1949) Comparing individual means in the analysis of variance. Biometrics 5(2):99–114
15. Ibrahim S, Khalid NEA, Manaf M (2010) Empirical study of brain segmentation using particle swarm optimization International Conference on Information Retrieval and Knowledge Management: 235-239 IEEE https://doi.org/10.1109/INFRKM.2010.5466910.
16. Ganesan R, Radhakrishnan S (2009) Segmentation of computed tomography brain images using genetic algorithm. Int J Soft Comput 4:157–161
17. Adams R, Bischof L (1994) Seeded region growing. IEEE Trans Pattern Anal Mach Intell 16:641–647. https://doi.org/10.1109/34.295913
18. Khalid NEA, Ibrahim Sand, Manaf M, Ngah UK (2010) Seed-based region growing study for brain abnormalities segmentation International Symposium on Information Technology 856-860 IEEE https://doi.org/10.1109/ITSIM.2010.5561560.
19. Azmi R, Norozi N, Anbiaee R, Salehi L, Amirzadi A (2011) IMPST: a new interactive self-training approach to segmentation suspicious lesions in breast MRI. J Med Signals Sens 1:138–148
20. Xi X, Shi H, Han L, Wang T, Ding HY, Zhang G, Yin Y (2017) Breast tumor segmentation with prior knowledge learning. Neurocomputing 237:145–157. https://doi.org/10.1016/j.neucom.2016.09.067
21. Feng Y, Dong F, Xia X, Chun Hong H, Fan Q, Hu Y, Gao M, Mutic S (2017) An adaptive Fuzzy C-means method utilizing neighboring information for breast tumor segmentation in ultrasound images. Med Phys 44(7):3752–3760. https://doi.org/10.1002/mp.12350
22. Patra DK, Si T, Mondal S, Mukherjee P (2021) Breast DCE-MRI segmentation for lesion detection by multi-level thresholding using student psychological based optimization. Biomed Signal Process Control 69:102925. https://doi.org/10.1016/j.bspc.2021.102925
23. Si T, Mukhopadhyay A (2021) Breast DCE-mri segmentation for lesion detection using clustering with fireworks algorithm. Proceedings of First Global Conference on Artificial Intelligence and Applications (GCAIA 2020), Springer, Singapore. https://doi.org/10.1007/978-981-33-4604-8

24. Kar B, Si T (2021) Breast DCE-MRI segmentation for lesion detection using clustering with Multi-verse optimization algorithm. In: Sharma TK, Ahn CW, Verma OP, Panigrahi BK (eds) Soft computing: theories and applications. Advances in Intelligent Systems and Computing, vol 1381. Springer, Singapore. https://doi.org/10.1007/978-981-16-1696-9_25
25. Patra DK, Mondal S, Mukherjee P (2021) Grammatical fireworks algorithm method for breast lesion segmentation in DCE-MRI. Int J Innov Technol Explor Eng 10(7):170–182. https://doi.org/10.35940/ijitee.G9054.0510721
26. Ha W (2021) Automatic breast tumor diagnosis in mri based on a hybrid cnn and feature-based method using improved deer hunting optimization algorithm. Comput Intell Neurosci 3:1–11. https://doi.org/10.1155/2021/5396327
27. Gihuijs KGA, Giger ML, Bick UA (1999) Method for computerized assessment of tumor extent in contrast-enhanced MR images of the breast. Computer Aid Diagn Med Imag 27(5):305–310
28. Benjelloun M, Adoui ME, Larhmam MA, Mahmoudi SA (2018) Auto-mated breast tumor segmentation in DCE-MRI using deep learning. 4th International Conference on Cloud Computing Technologies and Applications (Cloudtech) https://doi.org/10.1109/CloudTech.2018.8713352.
29. Liang X, Ramamohanara K, Frazer H, Yang Q (2012) Lesion Segmentation in Dynamic Contrast-Enhanced MRI of Breast International Conference on Digital Image Computing Techniques and Applications (DICTA), 1-8 IEEE https://doi.org/10.1109/DICTA.2012.6411734.
30. Zhang Y, Chan S, Chen J-H, Chang K-T, Lin C-Y, Pan H-B, Lin W-C, Kwong T, Parajuli R, Mehta RS, Chien S-H, Su M-Y (2021) Development of U-net breast density segmentation method for Fat-Sat MR images using transfer learning based on non-fat-sat model. J Digital Imaging. https://doi.org/10.1007/s10278-021-00472-z
31. Wang H, Cao J, Feng J, Xie Y, Yang D, Chen B (2021) Mixed 2D and 3D convolutional network with multi-scale context for lesion segmentation in breast DCE-MRI. Biomed Signal Process Control 68:102607. https://doi.org/10.1016/j.bspc.2021.102607
32. Tizhoosh HR (2005) Opposition-based learning: a new scheme for. Mach Intell I:695–701
33. Xu Q, Wang L, Wang N, Hei X, Zhao L (2014) A review of opposition-based learning from 2005 to 2012. Eng Appl Artif Intell 29:1–12
34. Rojas-Morales N, Rojas M-CR, Ureta EM (2017) A survey and classification of opposition-based metaheuristics. Computers Industrial Eng 110:424–435
35. Mahdavi S, Rahnamayana S, Deb K (2018) Opposition based learning: a literature review. Swarm Evolut Comput 39:1–23
36. Rahnamayan S, Tizhoosh HR, Salama MMA (2007) Quasi-oppositional differential evolution. IEEE Congr Evolut Comput. https://doi.org/10.1109/CEC.2007.4424748
37. Lingle W, Erickson BJ, Zuley ML, Jarosz R, Bonaccio E, Filippini J, Gruszauskas N (2007) Radiology Data from the Cancer Genome Atlas Breast Invasive Carcinoma Collection [TCGA-BRCA]
38. Clark K, Vendt B, Smith K, Freymann J, Kirby J, Koppel P, Moore S, Phillips S, Maffitt D, Pringle M, Tarbox L, Prior F (2013) The cancer imaging archive: maintaining and operating a public information repository. J Digit Imag 26(6):1045–1057
39. ME GM, Subashini MM (2019) Medical imaging with intelligent systems: a review Sangaiah, A.K. (ed.) Deep learning and parallel computing environment for bioengineering systems :53–73. Academic Press. Chap. 4. https://doi.org/10.1016/B978-0-12-816718-2.00011-7.
40. Mohan J, Krishnavenib V, Guo Y (2014) A survey on the magnetic resonance image denoising methods. Biomed Signal Process Control 9:56–69
41. Perona P, Malik J (1990) Scale-space and edge detection using anisotropic diffusion. IEEE Trans Pattern Anal Mach Intell 12(7):629–639
42. Balafar MA, Ramli AR, Mashohor S (2010) A new method for mr grayscale inhomogeneity correction. Artif Intell Rev 34:195–204
43. Shannon C, Weaver W (1964) The mathematical theory of communication. University of Illinois Press, Urbana, Ill
44. Soille P (1999) Morphological image analysis: principles and applications Proceedings of the First Conference on Visualization in Biomedical Computing 173-174 Springer-Verlag
45. Brown S, Tauler R, Walczak B (2020) Comprehensive chemometrics- chemical and biochemical data analysis, 2nd edn. Elsevier, Hoboken
46. Si T, Miranda P, Galdino JV, Nascimento A (2021) Grammar-based automatic programming for medical data classification: an experimental study. Artif Intell Rev. https://doi.org/10.1007/s10462-020-09949-9
47. Tawhid MA, Savsani V (2019) Multi-objective sine-cosine algorithm (MO-SCA) for multi-objective engineering design problems. Neural Comput Appl 31:915–929. https://doi.org/10.1007/s00521-017-3049-x
48. Derrac J, Garcia S, Molina D, Herrera F (2001) A practical tutorial on the use of nonparametric statistical tests as a methodology for comparing evolutionary and swarm intelligence algorithms. Swarm and Evolutionary Springer Nature 2021 LATEX template 40 Breast DCE-MRI segmentation using SMAQOBL Computation 1: 3–18
49. Tharwat A (2018) Classification assessment methods. Appl Comput Inform 17:168–192. https://doi.org/10.1016/j.aci.2018.08.003
50. Triantaphyllou E (2000) Multi-criteria decision making methods: a comparative study. Applied Optimization 44, 3rd edn. Springer. https://doi.org/10.1007/978-1-4757-3157-6.
51. Trelea IC (2002) The particle swarm optimization algorithm: convergence analysis and parameter selection. Information Process Lett 85:317–325